

---

# Advanced MR Techniques in Pediatric Neuroradiology: What Is Ready for Clinical Prime Time?

P. Ellen Grant

---

## Introduction

For an advanced MR technique to be ready for *clinical* prime time, (1) it must reliably detect abnormalities in individuals, not just provide statistical group differences; (2) processed images must be available rapidly; (3) acquisition times must be reasonable; and (4) time required by professional or supporting staff to create relevant images must be financially sustainable. Also ideally individual differences are visible on an image for the most rapid adaption in clinical practice. In this chapter diffusion imaging, MR spectroscopy, arterial spin labeling, fetal triplane reconstruction, and quantitative T1 and T2 imaging will be discussed, and examples where these sequences have clinical utility in individual pediatric patients will be provided.

---

## Diffusion Imaging

All major vendors provide sequences that perform diffusion-weighted imaging in at least six noncollinear and noncoplanar orientations and provide automatic online reconstruction of the following maps for interpretation:

1. Apparent diffusion coefficient (ADC) maps that provide voxel-based measures of the mean water diffusivity.
2. Fractional anisotropy (FA) maps with intensity representing the degree of coherence of water diffusion with increasing intensity representing greater coherence.
3. Color-coded FA maps representing the primary direction of water diffusion with the convention that blue represents water diffusion in the superior to inferior or inferior

to superior direction, red represents left to right or right to left diffusion, and green represents anterior to posterior or posterior to anterior diffusion.

4. Tractography images that provide information on the coherence of water diffusion over many voxels through reconstruction of “tracts.” If the same color coding as in the FA maps is used, blue fibers represent primarily projection fibers, red fibers represent primarily interhemispheric connections and fibers, and green fibers represent interhemispheric connections.

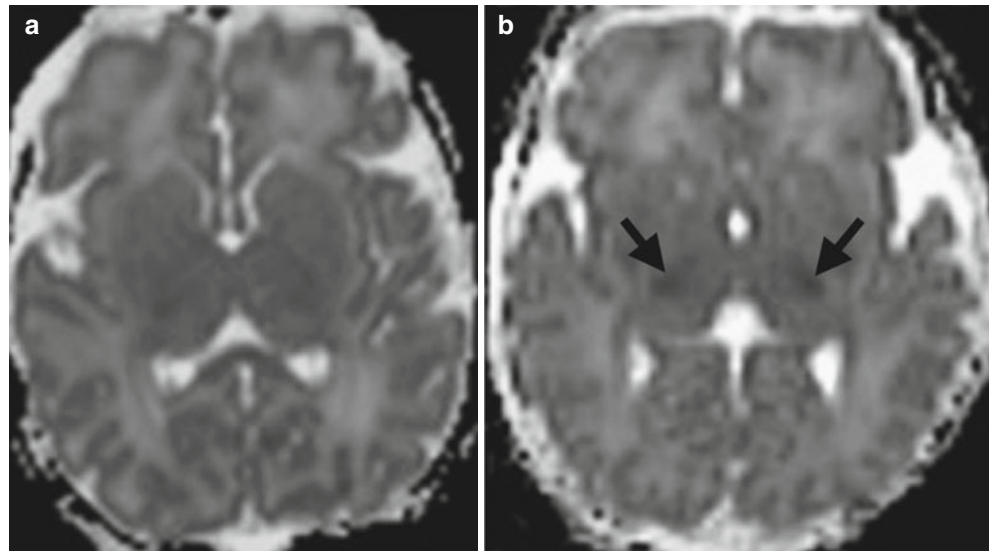
There are many different diffusion acquisition schemes and analysis approaches. The most common acquisition scheme used in clinical practice is the acquisition of 6–30 noncollinear and noncoplanar orientations at b values of 1000 s/mm<sup>2</sup> with up to one volume at  $b=0$  s/mm<sup>2</sup> for every six gradient directions. Newer acquisition methods such as simultaneous multislice (SMS) combined with parallel acquisition schemes and high-density phased-array coils at 3 T have significantly decreased acquisition times, allowing 35 gradient directions to be acquired in under 3 min [1]. Additional background on DTI principles can be found in many reviews articles [2–4].

The ability of ADC maps to detect acute ischemic events, metabolic compromise, collections of pus, and tumors with high cellular density in individual patients has been recognized for many years [5, 6]. In general, ADC maps are read visually informed by the individual reader’s knowledge of normal ADC values. In infants and young children, the regional variability and normal evolution of ADC values with brain maturation make interpretation of pediatric ADC maps challenging, particularly to those who do not read a high number of pediatric studies. There are references that provide general guidelines for regional ADC values with age, but typically only a few regions are reported or the focus is preterms and the entire reference data sets are not available [7–9]. There are emerging interactive atlases that will provide mean and standard deviations for ADC maps in normal infants and young children

---

P.E. Grant  
Departments of Radiology and Medicine, Boston Children’s Hospital and Harvard Medical School,  
300 Longwood Ave, Boston, MA 02115, USA  
e-mail: [Ellen.grant@childrens.harvard.edu](mailto:Ellen.grant@childrens.harvard.edu)

**Fig. 1** (a) Normal ADC map in a neonate. Note the regional variation in ADC values due to incomplete myelination. (b) ADC map in a neonate suffering from hypoxic ischemic encephalopathy (HIE). Arrows point to the abnormally low ADC values in the ventrolateral thalamus, a common area of injury when there is a short but significant loss of blood flow and oxygen to the neonatal brain. Note that in the normal neonate, this region is also slightly lower in ADC values than adjacent thalamus making it difficult in subtle cases to determine how low is abnormal



(e.g., <http://mi2b2beta.babymri.org/>). These interactive, high spatial and temporal density atlases are intended to guide clinical interpretation and help decrease the variance in clinical interpretations by providing a uniform reference standard. Such reference standards become helpful when interpreting neonatal ADC maps for evidence of hypoxic ischemic encephalopathy (Fig. 1).

The clinical interpretation of FA maps is less common but can provide highly relevant clinical information in certain clinical situations. In particular the presence of preserved FA in the context of decreased diffusion indicates preservation of tissue microstructure at the time of the image acquisition [10]. This information can be a helpful hint that a region of decreased diffusion may not be due to an evolving ischemic event but another mechanism such as metabolic compromise (Fig. 2) or tumor infiltration (Fig. 3).

Color FA maps are even less commonly viewed for clinical purposes but are often available for interpretation. These color maps may be helpful when trying to further assess preservation of tissue microstructure or characterize abnormal organization of major white matter tracts and different types of cerebral malformations such as brainstem and corpus callosum abnormalities (Fig. 4).

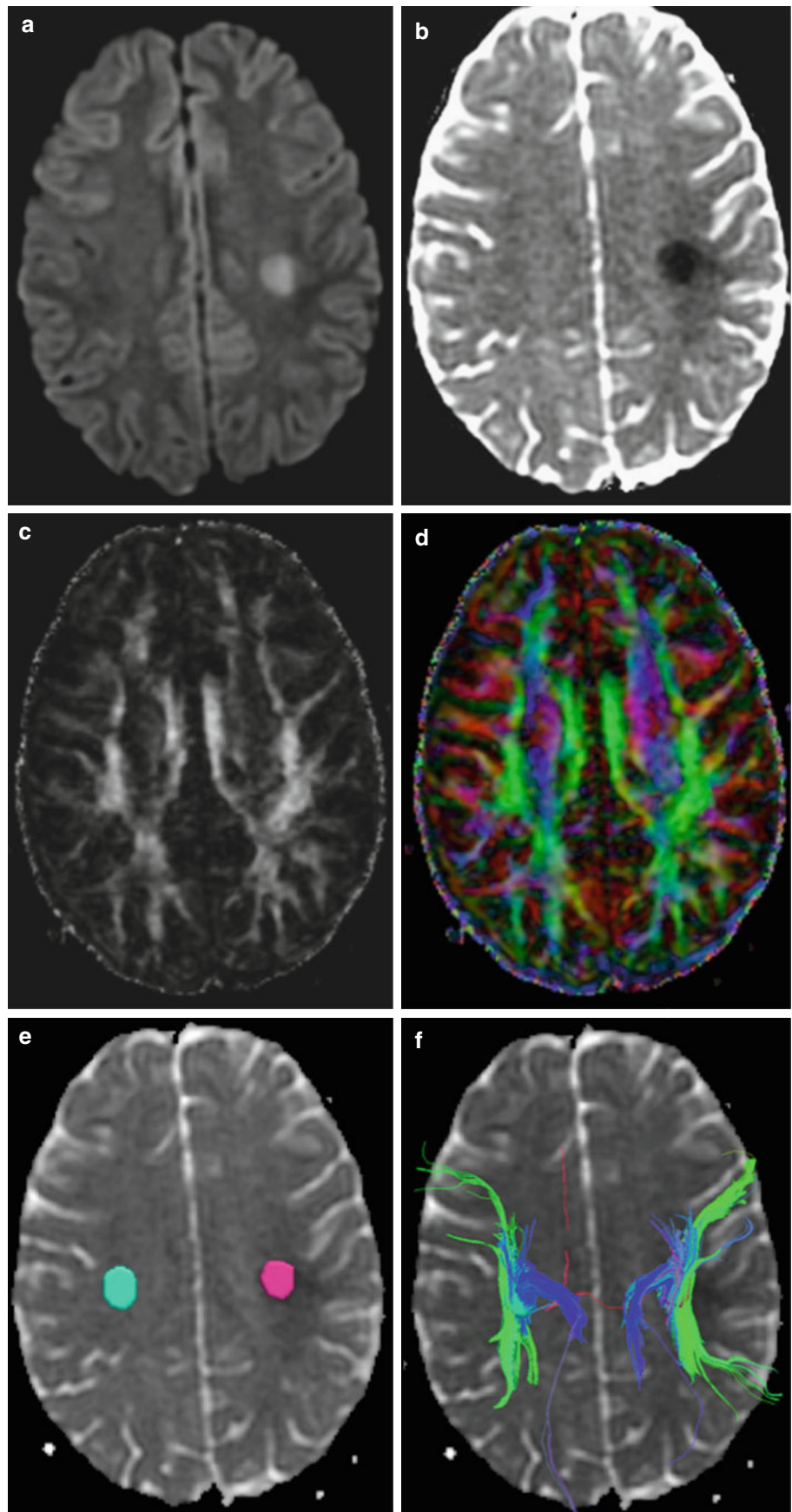
There are many tools and methods to create tractography images with many vendors now providing tools for tractography reconstruction on the MR console. As a result many radiologists can now easily perform tractography on clinical studies. Controversy over the utility of clinical tractography persists [11], but if the radiologist understands the limitations of the technique and does not over-interpret, useful information may be provided. For example, information regarding the displacement or involvement of specific white matter tracts may be helpful [12] (Figs. 2 and 3).

## MR Spectroscopy

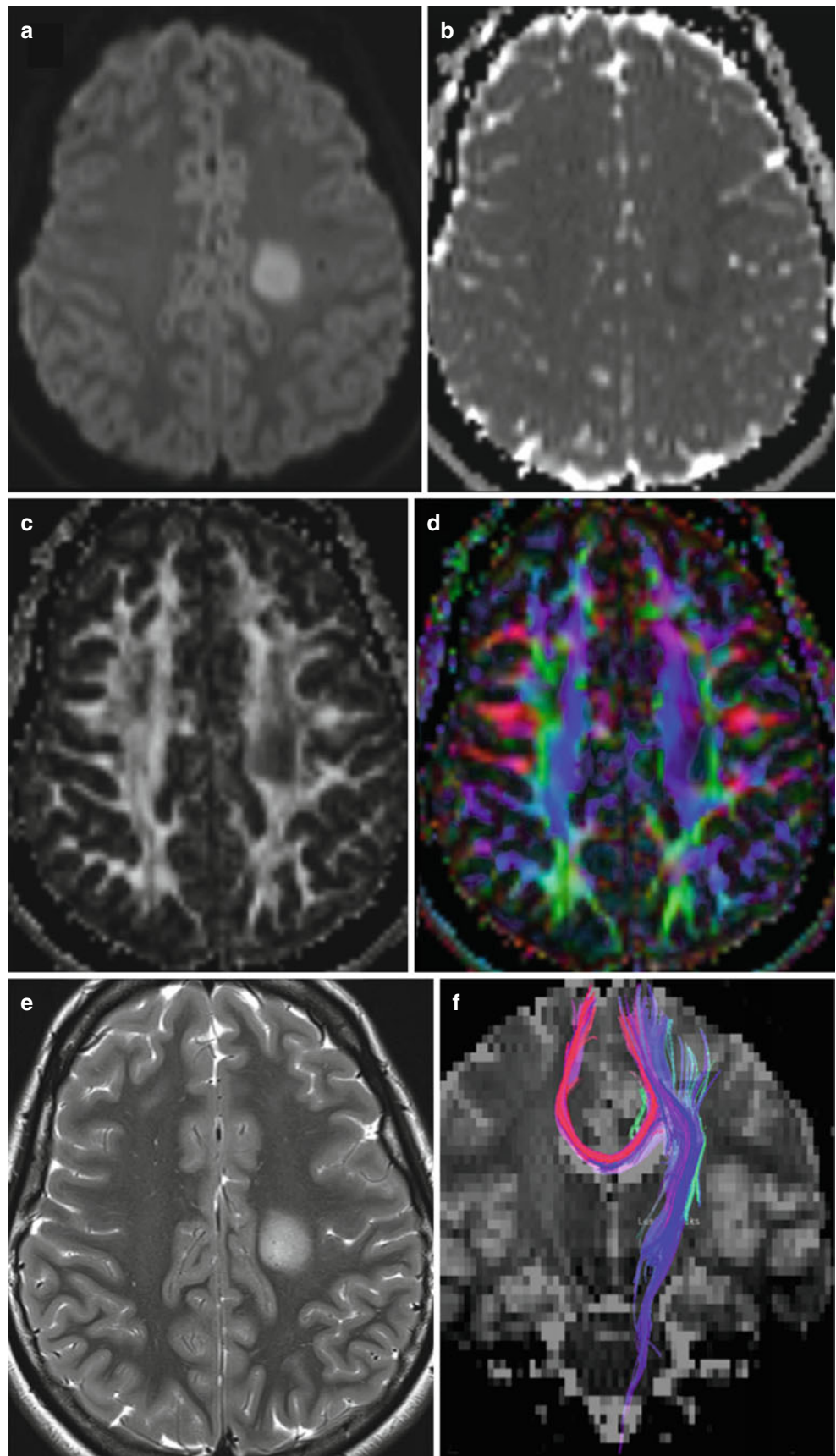
Proton ( $^1\text{H}$ ) MRS acquisition provides unique information about cerebral metabolites and has been proven useful in many pediatric applications such as hypoxic ischemic encephalopathy, metabolic disorders, tumors, demyelinating disorders, and trauma [13–16] (Fig. 5). The major brain metabolites feasible to assess clinically include myoinositol (mI), choline (Ch), creatine (Cr), glutamine and glutamate (glx), and N-acetylaspartate (NAA) with ratios to Cr as the most common approach. Many abnormal peaks are feasible to detect clinically and include lipids, lactate, glycine, alanine, pyruvate, succinate, valine, acetate, isoleucine, and leucine [16]. Absolute quantification of peaks requires additional technical expertise and additional software (most often LC Model) not available on clinical scanners. Separation of glutamine and glutamate requires longer scan times but is feasible; however, GABA requires much longer scan times at lower resolution as well as special editing techniques and is therefore not currently feasible for routine clinical studies.

Although now FDA approved, clinical application of MR spectroscopy has been limited by the ability to sample the same region in different imaging sessions, the lack of easy quantification, the lack of normal regional data at different TEs and different ages, as well as the time required for image acquisition. Newer 3D  $^1\text{H}$  MRS acquisition schemes provide multivoxel data making it possible to obtain regional measurements of major metabolites within 5 min (Fig. 6) [17]. The fact that these new methods can be co-registered to volumetric T1 images allows tracking of MRS changes over time. Although there is some information on the normal spectroscopy changes over time [18], the ability of 3D  $^1\text{H}$ -MRS to be registered to volumetric T1 images opens the door for future development of  $^1\text{H}$ -MRS atlases with regional information across development.

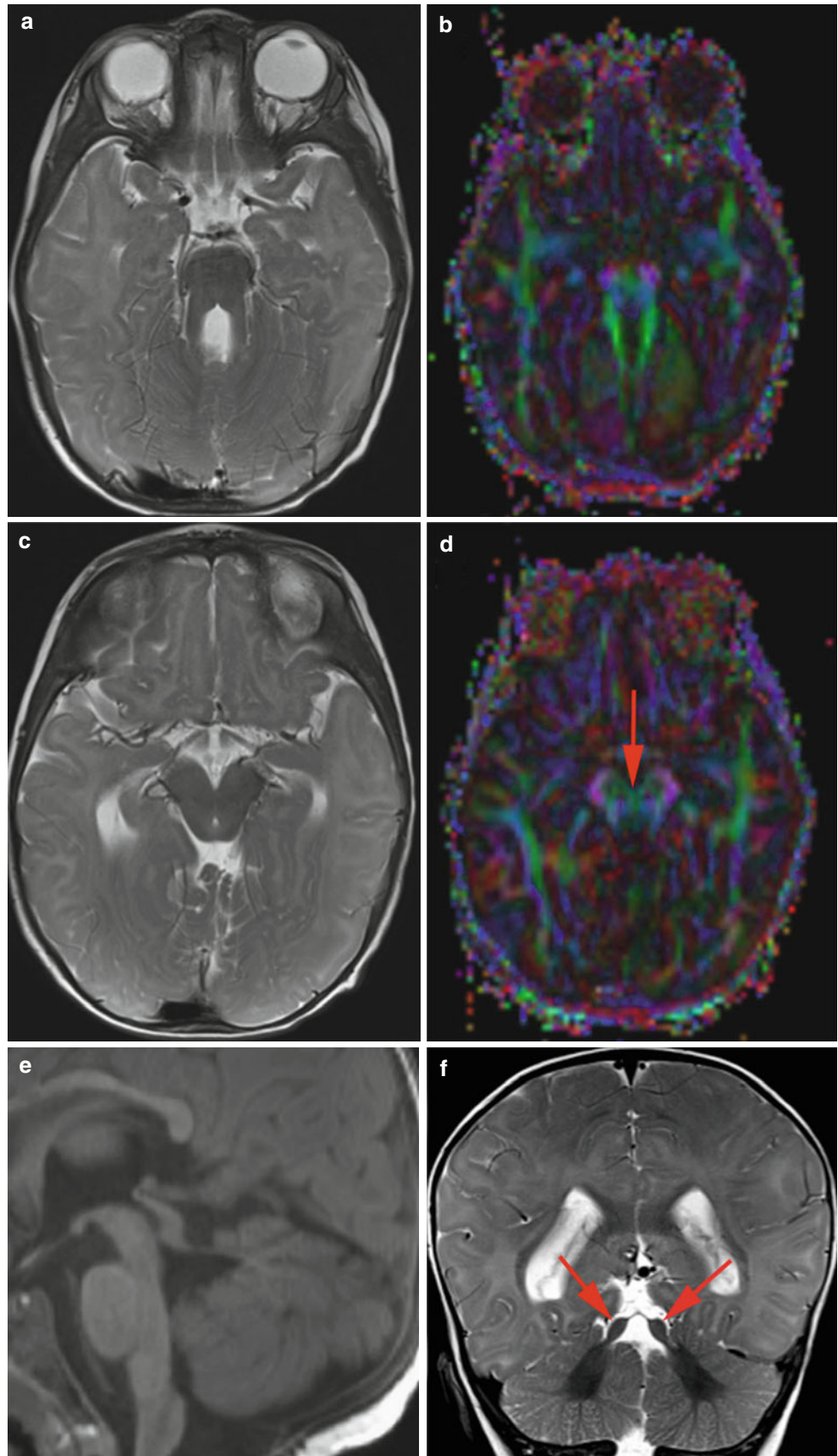
**Fig. 2** Young girl with acute lymphoblastic leukemia undergoing intrathecal methotrexate (MTX) therapy presenting with acute onset of right-sided weakness. (a) DWI and (b) ADC map shows a focal lesion with decreased diffusion. (c) FA map shows similar FA values in the lesion compared to the contralateral normal side. (d) Color FA map shows similar directions to the diffusion coherence as in the contralateral side. (e) ROIs were placed in the lesion and in the contralateral brain to generate tracts. (f) Tractography shows preservation of the long-range coherence and confirms that descending tracts, likely corticospinal tract, pass through the lesion. On the T2 images (not shown), the lesion was difficult to detect. The differential includes MTX toxicity, arterial ischemic stroke, or a demyelinating process. Given the clinical history of MTX therapy, this lesion likely corresponds to an area of metabolic compromise or white matter vacuolation with preservation of tissue microstructure at the time of the MRI. The child completely recovered



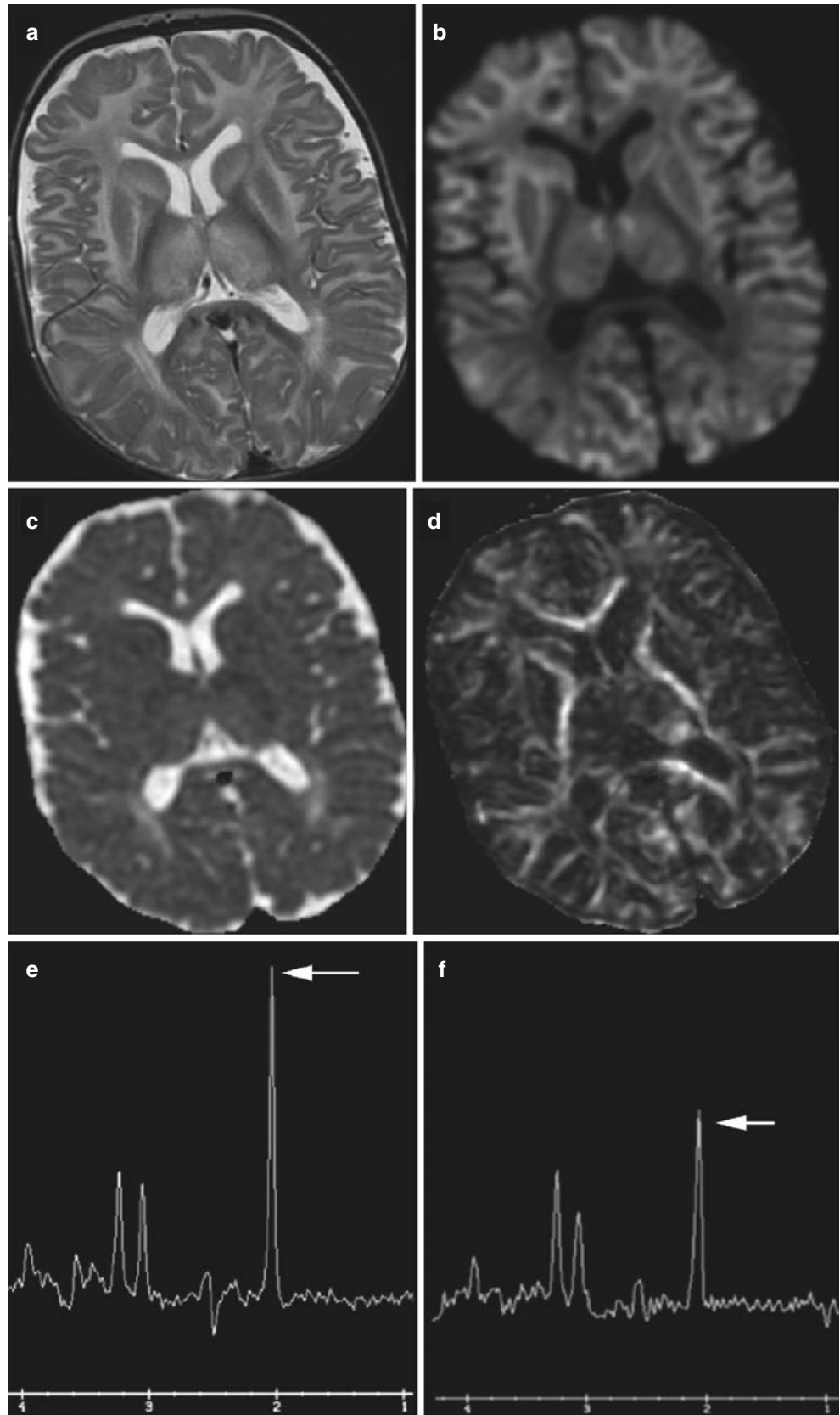
**Fig. 3** A 17-year-old girl presenting with new-onset right-sided weakness. (a) DWI and (b) ADC map show lesions with mixed ADC values. (c) FA map showed decreased FA and (d) color FA map shows similar diffusion directions as in the contralateral hemisphere. On the T2 image (e), the lesion has slightly ill-defined margins. (f) Tracks reconstructed using an ROI in the lesion show preservation of long-range coherence. The differential includes a demyelinating lesion or an infiltrative neoplasm. Over the next few months, the lesion continued to grow and was biopsied, revealing an infiltrating glioma grade III. As in this case, infiltrating neoplasms can decrease ADC due to increased cellularity and preserve overall tissue coherence



**Fig. 4** A 5-month-old female with intermittent apnea and hypoxia. (a) Axial T2 at the level of the superior cerebellar peduncles shows large superior cerebellar peduncles giving a molar tooth appearance. (b) Color FA map shows the green anterior-posterior direction of the axonal bundles. (c) Axial T2 at the level of the mid-brain appears normal but on (d) color FA map, the normal red spot indicating the decussation of the superior cerebellar peduncles is absent (*arrow*). (e) Hypoplastic and dysmorphic vermis and (f) coronal T2 showing enlarged superior cerebellar peduncles (*arrows*). The molar tooth appearance with lack of decussation of the superior cerebellar peduncles and small dysplastic vermis is diagnostic of Joubert syndrome



**Fig. 5** A 6-month-old presenting with a large head and hypotonia. (a) There is diffuse increased signal throughout the white matter on T2 with relative sparing of the corpus callosum and posterior limb internal capsule but involvement of the deep gray nuclei. (b) On DWI the white matter appears diffusely bright. (c) The ADC map is isointense despite the diffuse increased T2 seen throughout the white matter indicating that the edema is not extracellular. (d) FA values are normal to increased. (e) The patient's MRS has an elevated NAA peak (arrow) compared to (f) an age matched typically to a developing toddler. These findings are consistent with the diagnosis of Canavan disease with the white matter changes representing spongiform degeneration. The toddler had high urine N-Acetylaspartate, confirming the diagnosis



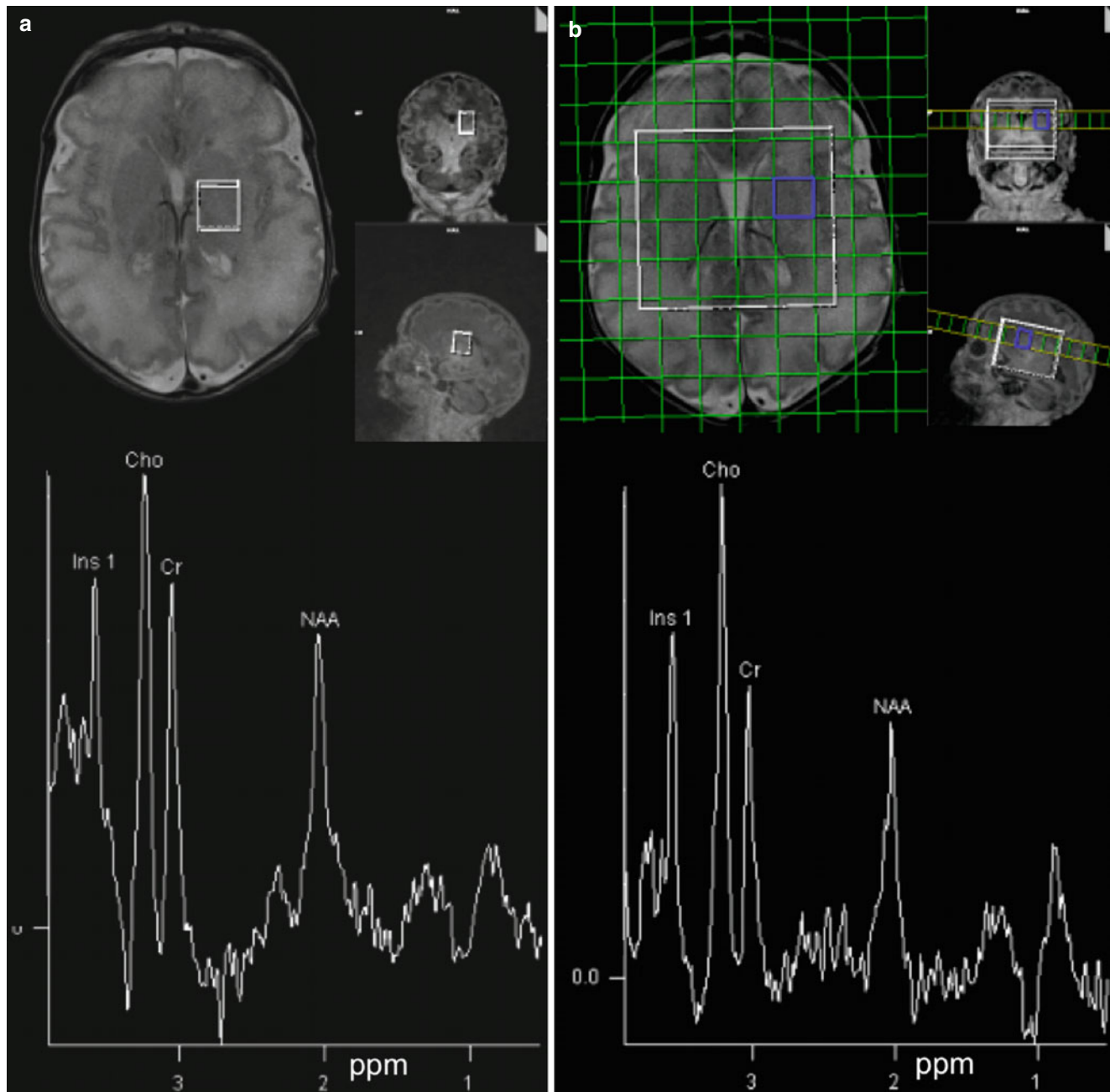


**Fig. 6** (a) Spectra from a 3 min single-voxel PRESS <sup>1</sup>H-MRS acquisition in one 3.4 cc voxel. (b) Spectra from a 3 min accelerated 3D spiral CSI <sup>1</sup>H-MRS acquisition providing 30 voxels of 2 cc volume to cover a

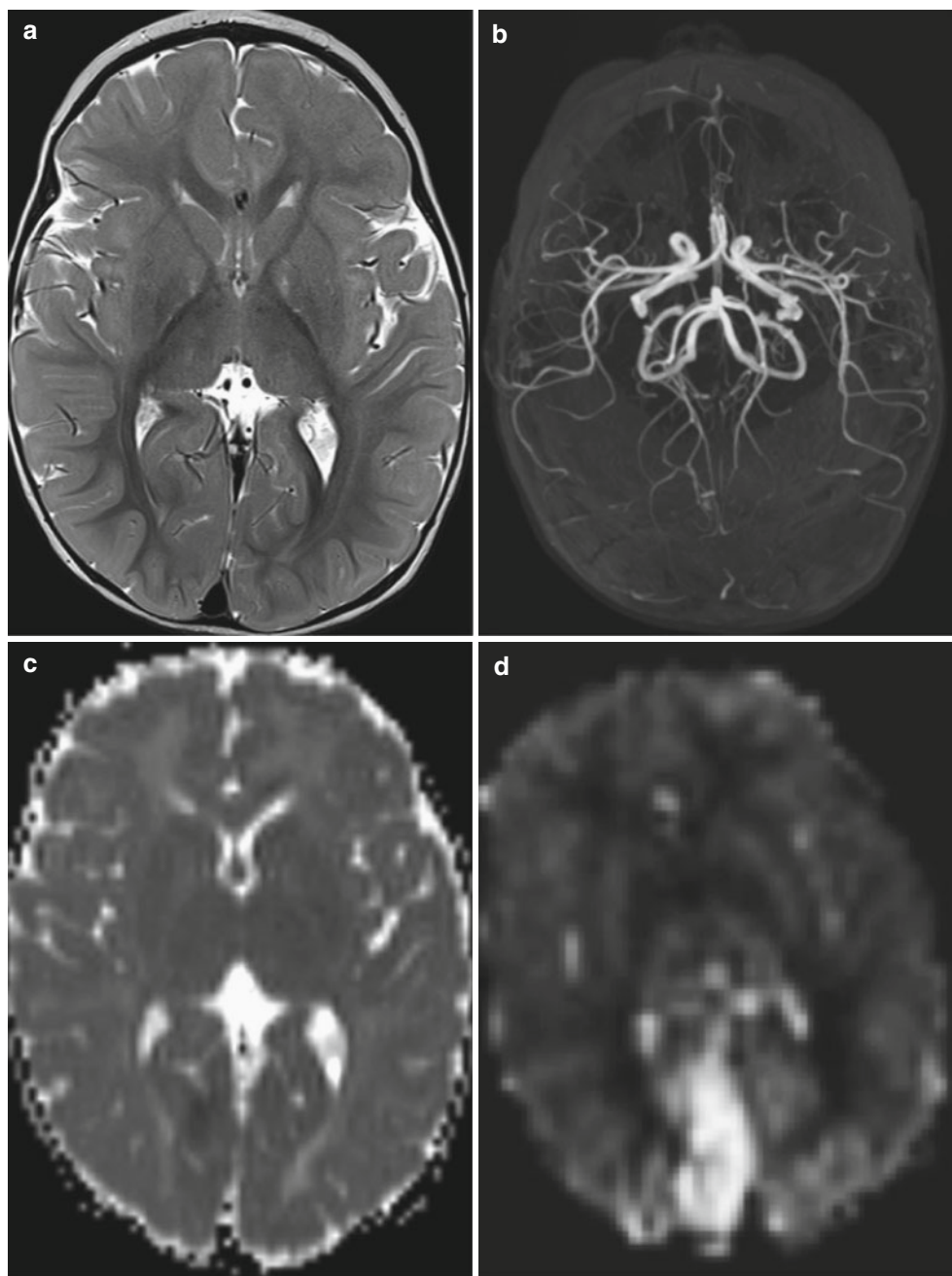
total of  $16 \times 16 \times 10$  cm regions with LASER-box excitation as shown by the box in the figure inset

## Arterial Spin Labeling

Arterial spin labeling (ASL) is a method for noninvasively labeling water molecules in flowing blood to assess cerebral parenchymal perfusion at the capillary level. In ASL inflowing arterial blood is labeled by one of many different methods. The most common labeling scheme on commercial scanners is pulsed ASL (PASL) where a short rf pulse is applied over a

volume in the neck. After a delay, designed to allow transit of labeled protons from the carotid and vertebral arteries into the capillaries and extra-axial space of the brain, images of the brain are acquired. The control images are obtained with no label and the two subtracted to provide a perfusion image. ASL is also a low signal-to-noise technique due to the small cerebral capillary vascular volume (5–6 %) and therefore requires multiple repetitions making it susceptible to motion

**Fig. 7** An 11-month-old girl presenting with epilepsy partialis continua. (a) Axial T2-weighted imaging was normal apart from subtle loss of gray white distinction in the right parasagittal occipital lobe. (b) Axial MIP from the 3D TOF MRA shows relative prominence of the right PCA compared to the right. (c) Subtle decreased ADC is evident in the right parasagittal occipital lobe. (d) Right parasagittal occipital lobe hyperperfusion is clearly visible on axial PASL. EEG revealed rhythmic high-amplitude delta with superimposed spikes (RHADS), a hallmark of Alpers' syndrome. The imaging findings are consistent with hyperperfusion and mild metabolic compromise from ongoing seizure activity. The child was confirmed to have a POLG1 mutation



artifacts. ASL is a T1-based technique and therefore must be performed prior to contrast administration. Further details on ASL methods can be found in review articles [19, 20].

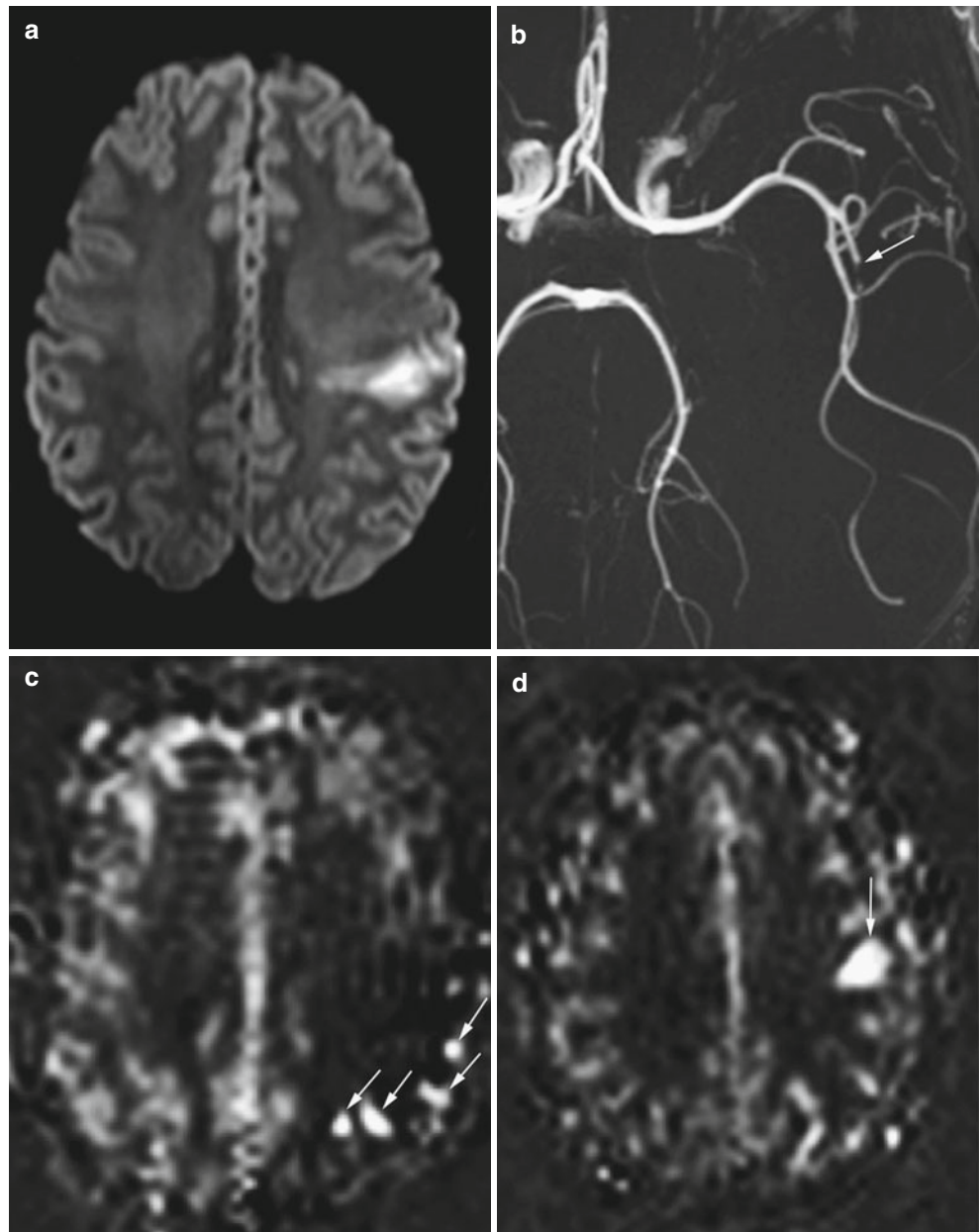
Controversy exists over ability of ASL methods to provide accurate quantitation of cerebral perfusion due to the need to know the T1 of blood, the labeling efficiency, and label delay, as well as the need to control for magnetization transfer effects [19]. In pediatric imaging many of these factors vary making quantitation even more challenging than in adults. However, despite these issues, numerous articles describing the potential clinical utility exist [20–25], and in

addition a consensus article providing guidance to optimizing ASL across vendors is available [26].

Due to the above noted issues with absolute quantitation, clinical applications of ASL are most robust when assessing regional changes in cerebral perfusion. Such changes in cerebral perfusion are extremely useful in identifying alterations in cerebral perfusion in symptomatic patients when no structural abnormalities are identified or in further characterizing an abnormality visible on other sequences. Abnormal increases or decreases in regional cerebral perfusion can be driven by (1) alterations in regional demand, typically due to



**Fig. 8** (a) DWI showing decreased diffusivity from an acute arterial ischemic stroke in the left MCA territory. (b) On the 3D TOF MRA, loss of flow-related enhancement is detected in the superior division of the left MCA (*arrow*). (c) Initial PASL at presentation shows a region of hypoperfusion is larger region than the DWI lesion indicating a penumbra. High signal in the vessels occurs due to delayed arrival of label (*arrows*). (d) After TPA, the PASL now shows near-complete resolution of the region of hypoperfusion with now a focal region of parenchymal hyperperfusion (*arrow*)



alterations in regional neural activity (Fig. 7), or (2) regional abnormalities of the vascular system related to vascular anomalies, ischemic events, neovascularization in tumors, arteriovenous fistulas, etc. (Fig. 8).

### Fetal Triplane Imaging

Single-shot T2-weighted images such as HASTE or SSFSE are used in sagittal, coronal, and axial planes for clinical evaluation of the fetal brain. Due to motion

degradation of slices, these acquisitions are often not exactly in the desired plane and often not exactly orthogonal. Many groups have developed post-processing approaches to combine the three planes together to create a coherent higher resolution 3D brain volume (Fig. 9) [27–30], but these methods currently require manual intervention and many hours of computational time. In addition most tools fail approximately 50 % of the time due to poor image quality as a result of motion or image artifacts. As a result such much needed tools for clinical fetal imaging are not yet available.

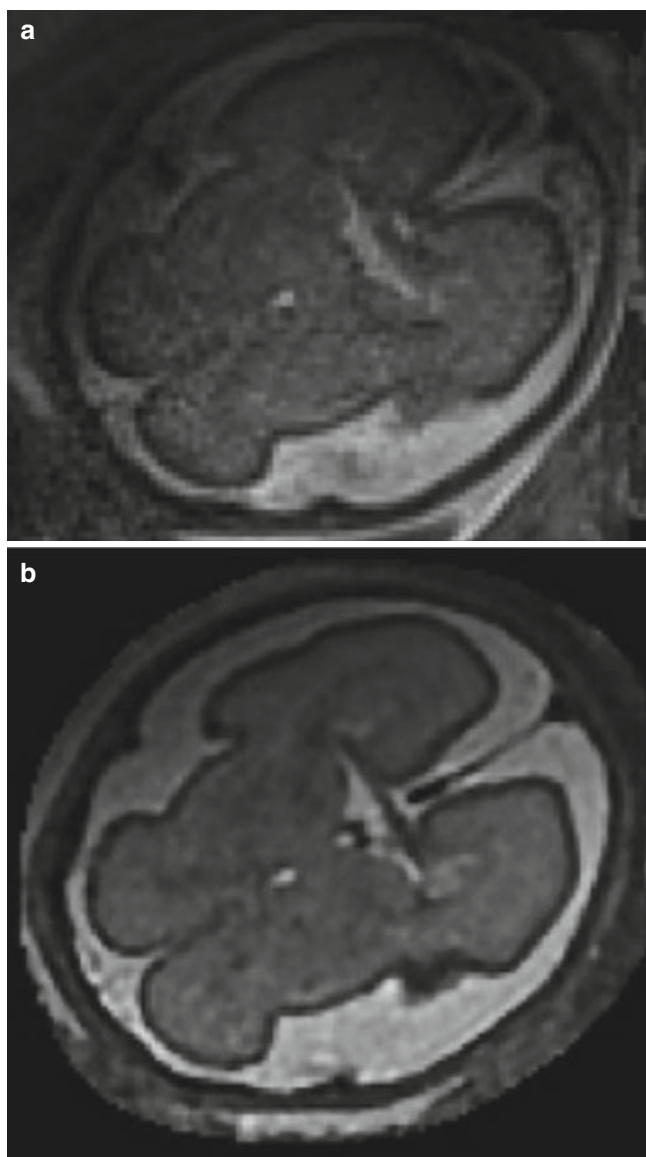


**Fig. 9** (a) One axial HASTE image of a fetal brain. (b) Axial image through a synthesized volume of a fetal brain that is higher in resolution and has less motion degradation after an offline super-resolution reconstruction using as input multiple orthogonal HASTE acquisitions

### Quantitative T1 and T2

In the quest for more accurate lesion detection, particularly in children with focal epilepsy, there is a continual push to improve image resolution and contrast as detection of focal

cortical lesions significantly improves surgical outcomes and confirmation of multiple lesions in the same clinical context will prompt a more thorough evaluation before surgical resection is attempted. With 32-channel phased-array coils now commonly available at 3 T, image quality has significantly improved with 1 mm isotropic T1-weighted and FLAIR T2 volumetric acquisitions commonly performed in combination with 2 mm-thick T2 TSE images with high in-plane resolution. However, as the search for lesions intensifies, subtle differences in cortical signal due to variations in proximity to the phased-array coils can prove challenging. This has led the desire for quantitative T1- and T2-weighted imaging.

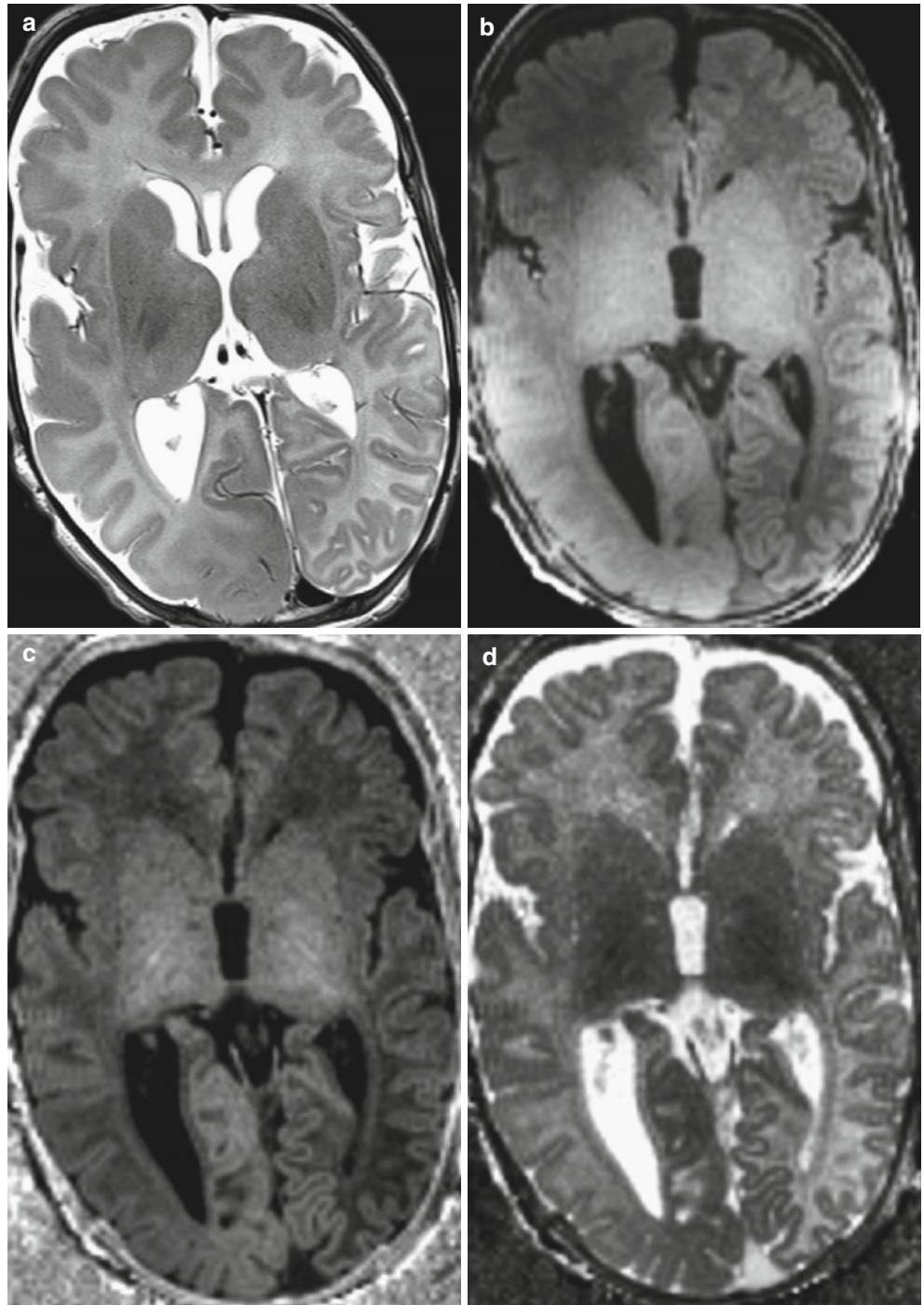
Sequences that provide estimates of T1 with automatically reconstructed T1 maps for visual inspection such as MPXRAGE are becoming commercially available. Such sequences remove signal intensity biases due to the reception profiles of the coils and assist in the visual detection of focal lesions. Sequences that provide estimates of T2 are also available on some systems; however, the application of such sequences is limited by the long acquisition times required (~10 min) but may be clinically justified in complex epilepsy cases as a second-line evaluation (Fig. 10).

### Summary

Although there is still progress to be made, many advanced techniques are becoming integrated into the workflow of clinical pediatric neuroradiology. Over-interpretation and definitive statements regarding processed data can be misleading and dangerous. Therefore, these advanced techniques require the neuroradiologist to understand the breadth of physiologies and pathophysiologies that can alter signal intensity or a processed result as well as the potential artifacts that can lead to misleading results.

In the past, quantitation has been viewed with skepticism, but as our tools improve, neuroradiologists need to be open-minded about the potential of quantitative neuroimaging. However, as the field is being pushed toward standardization and quantitation, there will be an increasing need to provide normative measures across development that will require collaboration and incorporation of data from multiple sites with access to patient populations of different ethnic and environmental backgrounds.

**Fig. 10** A 7-week-old infant presenting with fever and concern for sepsis followed by persistent seizure activity. **(a)** Axial T2 shows an asymmetrically large right hemisphere with an enlarged genu of the corpus callosum. T2 signal throughout the right hemisphere white matter is abnormally low and there is apparent thickening of the cortex diffusely. The left temporal and occipital lobe looks normal but the right frontal lobe is concerning for involvement. **(b)** Axial reformation of a sagittal MPRAGE has nonuniform signal due to the phased-array coils making further evaluation of the left frontal lobe difficult. **(c)** Axial reformation of the uniform intensity image created from the MP2RAGE acquisition shows subtle differences in white matter signal in the left frontal and occipital lobe. **(d)** Axial reformation of the T1 map created from the MP2RAGE acquisition confirms the abnormal T1 values in the left frontal white matter compared to the occipital lobe and more similar to the right frontal lobe. These findings are consistent with right hemimegalencephaly with additional involvement of the left frontal lobe



## References

1. Setsompop K, Cohen-Adad J, Gagoski BA, Raij T, Yendiki A, Keil B et al (2012) Improving diffusion MRI using simultaneous multi-slice echo planar imaging. *Neuroimage* 63(1):569–580
2. Mori S, Zhang J (2006) Principles of diffusion tensor imaging and its applications to basic neuroscience research. *Neuron* 51(5):527–539
3. Basser PJ, Jones DK (2002) Diffusion-tensor MRI: theory, experimental design and data analysis – a technical review. *NMR Biomed* 15(7–8):456–467
4. Hagmann P, Jonasson L, Maeder P, Thiran JP, Wedeen VJ, Meuli R (2006) Understanding diffusion MR imaging techniques: from scalar diffusion-weighted imaging to diffusion tensor imaging and beyond. *Radiographics* 26(Suppl 1):S205–S223
5. Schaefer PW, Grant PE, Gonzalez RG (2000) Diffusion-weighted MR imaging of the brain. *Radiology* 217(2):331–345
6. Grant PE, Matsuda KM (2003) Application of new MR techniques in pediatric patients. *Magn Reson Imaging Clin N Am* 11(3):493–522
7. Nossin-Manor R, Card D, Morris D, Noormohamed S, Shroff MM, Whyte HE et al (2013) Quantitative MRI in the very preterm brain: assessing tissue organization and myelination using magnetization transfer, diffusion tensor and T(1) imaging. *Neuroimage* 64:505–516
8. Sadeghi N, Prastawa M, Fletcher PT, Wolff J, Gilmore JH, Gerig G (2013) Regional characterization of longitudinal DT-MRI to study white matter maturation of the early developing brain. *Neuroimage* 68:236–247
9. Miller JH, McKinsty RC, Philip JV, Mukherjee P, Neil JJ (2003) Diffusion-tensor MR imaging of normal brain maturation: a guide to structural development and myelination. *AJR Am J Roentgenol* 180(3):851–859
10. Grant PE, He J, Halpern EF, Wu O, Schaefer PW, Schwamm LH et al (2001) Frequency and clinical context of decreased apparent diffusion coefficient reversal in the human brain. *Radiology* 221(1):43–50
11. Pujol S, Wells W, Pierpaoli C, Brun C, Gee J, Cheng G et al (2015) The DTI challenge: toward standardized evaluation of diffusion tensor imaging tractography for neurosurgery. *J Neuroimaging* 25(6):875–882
12. Campanella M, Ius T, Skrap M, Fadiga L (2014) Alterations in fiber pathways reveal brain tumor typology: a diffusion tractography study. *PeerJ* 2, e497
13. Panigrahy A, Nelson MD Jr, Bluml S (2010) Magnetic resonance spectroscopy in pediatric neuroradiology: clinical and research applications. *Pediatr Radiol* 40(1):3–30
14. Cecil KM (2006) MR spectroscopy of metabolic disorders. *Neuroimaging Clin N Am* 16(1):87–116, viii
15. Cecil KM (2013) Proton magnetic resonance spectroscopy: technique for the neuroradiologist. *Neuroimaging Clin N Am* 23(3):381–392
16. Oz G, Alger JR, Barker PB, Bartha R, Bizzi A, Boesch C et al (2014) Clinical proton MR spectroscopy in central nervous system disorders. *Radiology* 270(3):658–679
17. Yazbek S, Prabhu SP, Connaughton P, Grant PE, Gagoski B (2015) Comparison of accelerated 3-D spiral chemical shift imaging and single-voxel spectroscopy at 3T in the pediatric age group. *Pediatr Radiol* 45(9):1417–1422
18. Bluml S, Wisnowski JL, Nelson MD Jr, Paquette L, Gilles FH, Kinney HC et al (2013) Metabolic maturation of the human brain from birth through adolescence: insights from in vivo magnetic resonance spectroscopy. *Cereb Cortex* 23(12):2944–2955
19. Petersen ET, Zimine I, Ho YC, Golay X (2006) Non-invasive measurement of perfusion: a critical review of arterial spin labelling techniques. *Br J Radiol* 79(944):688–701
20. Deibler AR, Pollock JM, Kraft RA, Tan H, Burdette JH, Maldjian JA (2008) Arterial spin-labeling in routine clinical practice, part 1: technique and artifacts. *AJNR Am J Neuroradiol* 29(7):1228–1234
21. Amukotuwa SA, Yu C, Zaharchuk G (2016) 3D Pseudocontinuous arterial spin labeling in routine clinical practice: A review of clinically significant artifacts. *J Magn Reson Imaging* 43(1):11–27
22. Deibler AR, Pollock JM, Kraft RA, Tan H, Burdette JH, Maldjian JA (2008) Arterial spin-labeling in routine clinical practice, part 2: hypoperfusion patterns. *AJNR Am J Neuroradiol* 29(7):1235–1241
23. Deibler AR, Pollock JM, Kraft RA, Tan H, Burdette JH, Maldjian JA (2008) Arterial spin-labeling in routine clinical practice, part 3: hyperperfusion patterns. *AJNR Am J Neuroradiol* 29(8):1428–1435
24. Petcharunpaisan S, Ramalho J, Castillo M (2010) Arterial spin labeling in neuroimaging. *World J Radiol* 2(10):384–398
25. Telischak NA, Detre JA, Zaharchuk G (2015) Arterial spin labeling MRI: clinical applications in the brain. *J Magn Reson Imaging* 41(5):1165–1180
26. Alsop DC, Detre JA, Golay X, Gunther M, Hendrikse J, Hernandez-Garcia L et al (2015) Recommended implementation of arterial spin-labeled perfusion MRI for clinical applications: a consensus of the ISMRM perfusion study group and the European consortium for ASL in dementia. *Magn Reson Med* 73(1):spcone
27. Tourbier S, Bresson X, Hagmann P, Thiran JP, Meuli R, Cuadra MB (2015) An efficient total variation algorithm for super-resolution in fetal brain MRI with adaptive regularization. *Neuroimage* 118:584–597
28. Rousseau F, Kim K, Studholme C, Koob M, Dietemann JL (2010) On super-resolution for fetal brain MRI. *Med Image Comput Assist Interv* 13(Pt 2):355–362
29. Gholipour A, Estroff JA, Barnewolt CE, Connolly SA, Warfield SK (2011) Fetal brain volumetry through MRI volumetric reconstruction and segmentation. *Int J Comput Assist Radiol Surg* 6(3):329–339
30. Kuklisova-Murgasova M, Quaghebeur G, Rutherford MA, Hajnal JV, Schnabel JA (2012) Reconstruction of fetal brain MRI with intensity matching and complete outlier removal. *Med Image Anal* 16(8):1550–1564